

Estimating Fold Changes from Partially Observed Outcomes with Applications in Microbial Metagenomics

David S Clausen

and

Amy D Willis*

Department of Biostatistics, University of Washington

9 February 2024

Abstract

We consider the problem of estimating fold-changes in the expected value of a multivariate outcome that is observed subject to unknown sample-specific and category-specific perturbations. We are motivated by high-throughput sequencing studies of the abundance of microbial taxa, in which microbes are systematically over- and under-detected relative to their true abundances. Our log-linear model admits a partially identifiable estimand, and we establish full identifiability by imposing interpretable parameter constraints. To reduce bias and guarantee the existence of parameter estimates in the presence of sparse observations, we apply an asymptotically negligible and constraint-invariant penalty to our estimating function. We develop a fast coordinate descent algorithm for estimation, and an augmented Lagrangian algorithm for estimation under null hypotheses. We construct a model-robust score test, and demonstrate valid inference even for small sample sizes and violated distributional assumptions. The flexibility of the approach and comparisons to related methods are illustrated via a meta-analysis of microbial associations with colorectal cancer.

1 Introduction

Communities of microorganisms known as microbiomes have become a focus of study across multiple scientific disciplines, including in many areas of human health and disease (Young, 2017; Yamashita and Takeshita, 2017; Shreiner et al., 2015; Moffatt and Cookson, 2017). Modern microbiome research leans heavily on high-throughput sequencing techniques, which enable researchers to identify large numbers of microbial taxa on the basis of genetic material detected in a given environment. In this paper, we consider the problem of making statistical statements about changes in

*Contact: adwillis@uw.edu. The authors gratefully acknowledge support from the National Institute of General Medical Sciences (R35 GM133420). The authors are grateful to Sarah Teichman for thoughtful suggestions on the manuscript and code.

the “absolute” concentrations of microbes in an environment using only the “relative” information provided by marker gene and whole genome shotgun sequencing. Our approach also accounts for the observation that different microbes are consistently over- or under-counted (McLaren et al., 2019).

Most generally, this paper introduces a method for inference on ratios of means of a nonnegative multivariate outcome observed only up to unknown sample-specific and category-specific scaling terms. To our knowledge no similar methods currently exist, but a related niche in microbiome science is occupied by a range of regression models that rely on log-ratio transformations to target a similar estimand. These include ANCOM and its variants, which attempt to distinguish sampling, structural, and “outlier” zero values in high-throughput sequencing data prior to transformation and modeling (Mandal et al., 2015; Kaul et al., 2017; Lin and Peddada, 2020); and ALDEx2, which employs a Bayesian approach to impute nonzero values before transformation (Fernandes et al., 2014).

ANCOM and ALDEx2 fall into the larger category of “differential abundance” methods, which include LefSe, DESeq2, edgeR, metagenomeSeq, IFAA, and corncob (Segata et al., 2011; Love et al., 2014; Robinson et al., 2010; Paulson et al., 2013; Li et al., 2021; Martin et al., 2020), as well as many others (see Nearing et al. (2022) for a recent empirical comparison). DESeq2 and edgeR were originally developed for RNAseq data and attempt to address excess-Poisson dispersion via a negative binomial likelihood (Love et al., 2014; Robinson et al., 2010). By contrast, metagenomeSeq was developed specifically for microbiome analysis and employs a zero-inflated Gaussian model motivated by the high degree of sparsity in microbiome datasets (Paulson et al., 2013). LefSe, also developed for microbiome analysis, attempts to identify “metagenomic biomarkers” via a Kruskal-Wallis test followed by Wilcoxon tests on normalized sequencing data (Segata et al., 2011), and IFAA fits a log-linear zero-inflated Gaussian model by identifying a reference taxon whose abundance is conditionally independent of covariates (Li et al., 2021). Corncob (Martin et al., 2020) models both taxon relative abundances and dispersion of relative abundances via a beta-binomial model with logit link functions. We note that although the regression models above are all referred to as differential abundance methods (Nearing et al., 2022), they do not target a common estimand and hence do not produce strictly comparable inference. Furthermore, most of these methods target estimands defined in terms of microbial proportions, while our approach targets an estimand defined on the total microbial abundance scale (e.g., taxon-specific cell counts, DNA concentration, or copy number).

Our manuscript is structured as follows: we introduce our model and establish identifiability of equivalence classes of parameters in Section 2. We discuss estimation via a generalized estimating equations framework in Section 3, and inference via model misspecification-robust testing in Section 4. We present simulation results pertaining to Type 1 and 2 error rates in Section 5 and consider a data analysis in Section 6. We conclude with a discussion in Section 7. Open-source software implementing the method is available at github.com/statdivlab/radEmu, and code to reproduce the analyses are available at github.com/statdivlab/radEmu_supplementary.

2 Model

2.1 Motivation

Our work is motivated by settings in which an “ideal” dataset $W_{ij} \geq 0$ (samples $i = 1, \dots, n$ and categories $j = 1, \dots, J$) is not observed, but a distorted proxy $Y_{ij} \geq 0$ is available. Observing Y rather than W represents a loss of information in two critical ways. Firstly, the magnitude of $Y_i \in \mathbb{R}_{\geq 0}^J$ is uninformative with respect to the magnitude of $W_i \in \mathbb{R}_{\geq 0}^J$. In addition, the composition of Y_i may be systematically distorted relative to W_i as a result of differential detection. That is, observations from category j_1 may be more readily observed than observations from category j_2 , and the magnitude of the detection effects are unknown. Our goal is to estimate fold-differences in $\mathbb{E}W_{\cdot j}$ across covariates, that is, $\mathbb{E}W_{\{i: X_i=x\}j} / \mathbb{E}W_{\{i: X_i=x'\}j}$. We formalize our model and approach to estimating fold-differences in Section 2.2.

We our motivating example of microbial communities, W_{ij} represents the (unobserved) cell or DNA concentration of microbial taxon j in sample i , which are prohibitively time- and labor-intensive to observe for all taxa $j = 1, \dots, J$ (Williamson et al., 2022). However, it is relatively straightforward to perform high-throughput sequencing to produce data Y_{ij} , such as the (observed) read depth of taxon j in sample i in shotgun sequencing, or the number of times sequence variant j is observed in sample i based on amplicon sequencing. In the case-control microbiome studies considered in Section 6, we are interested in estimating the fold-difference in the mean cell concentration of taxa j when comparing cases to otherwise similar controls.

2.2 Model statement and parameter identifiability

Suppose that for pairs (X_i, W_i) with $X_i \in \mathbb{R}^p$ and $W_i \in \mathbb{R}_{\geq 0}^J$,

$$\log \mathbb{E}[W_i | X_i, \beta^*] = X_i \beta^*. \quad (1)$$

Our target of inference is $\beta^* \in \mathbb{R}^{p \times J}$. Unfortunately, however, we do not observe W_i , and so we cannot directly estimate β^* via (1). Instead, we instead observe a perturbed outcome $Y_i \in \mathbb{R}_{\geq 0}^J$ such that

$$\log \mathbb{E}[Y_i | X_i, \beta^*, z_i, \delta] = z_i \mathbf{1}_J^T + X_i \beta^* + \delta^T, \quad (2)$$

where sample-specific scalings $z_i \in \mathbb{R}$ and category-specific detection effects $\delta \in \mathbb{R}^J$ are unknown. Hence, the mean of Y_{ij} is equal to the mean of W_{ij} subject to scaling by the sample-specific factor $\exp(z_i)$ and category-specific factor $\exp(\delta_j)$.

As our target of inference is β^* , we consider $\mathbf{z} = [z_1, \dots, z_n]^T$ and δ as nuisance parameters. δ is straightforward to address if $\mathbf{1}_n$ lies in the column space of $\mathbf{X} = [X_1^T, \dots, X_n^T]^T$, as is typically the case in practice. Without loss of generality, we define $\mathbf{X} = [\mathbf{1}_n \ \mathbf{D}] \in \mathbb{R}^{n \times p}$ and $\mathbf{Y} = [Y_1^T, \dots, Y_n^T]^T \in \mathbb{R}^{n \times J}$, and rewrite model (14) as follows:

$$\log \mathbb{E}[\mathbf{Y} | \mathbf{X}] = \mathbf{z} \mathbf{1}_J^T + \mathbf{1}_n \beta_0 + \mathbf{D} \beta^{*(-0)} = \mathbf{z} \mathbf{1}_J^T + \mathbf{X} \beta \quad (3)$$

for $\beta_0 = \beta_0^* + \delta^T$ and $\beta = [\beta_0^T, \beta_1^{*T}, \dots, \beta_{p-1}^{*T}]^T$, for $\beta_k^* \in \mathbb{R}^{1 \times J}$ the $k + 1$ -th row of β^* . In particular, because β_0 depends on the nuisance detection effects δ , it has no scientifically meaningful interpretation, but $\beta_1, \dots, \beta_{p-1}$ contain useful information regarding $\beta_1^*, \dots, \beta_{p-1}^*$, as discussed in more detail below.

We now turn our attention to \mathbf{z} , which is not identifiable under our model because for any $\alpha \in \mathbb{R}^p$, we have that

$$z_i \mathbf{1}_J^T + X_i(\beta + \alpha \mathbf{1}_J^T) = z_i^\dagger \mathbf{1}_J^T + X_i \beta \quad (4)$$

for $z_i^\dagger := (z_i + X_i \alpha)$. Hence if $\beta^\dagger = \beta + \alpha \mathbf{1}_J^T$ for some $\alpha \in \mathbb{R}^p$, we can always find a $z_i^\dagger \in \mathbb{R}$ such that

$$\log \mathbb{E}[Y_i | X_i, \beta, z_i] = \log \mathbb{E}[Y_i | X_i, \beta^\dagger, z_i^\dagger], \quad (5)$$

and therefore mean function (14) is not identifiable in β and z_i . However, mean function (14) is *partially identifiable* because we can define equivalence classes of β 's such that for β and β^\dagger in the same equivalence class, there always exist z_i and z_i^\dagger such that (5) holds, and for β and β^\dagger in distinct classes, there never exist such z_i and z_i^\dagger . We now make the form of these classes explicit and show that they have the properties discussed above.

Lemma 1. For arbitrary $b \in \mathbb{R}^{p \times J}$, define

$$G_b = \{\beta \in \mathbb{R}^{p \times J} : \beta = b + \alpha \mathbf{1}_J^T \text{ for some } \alpha \in \mathbb{R}^p\}.$$

If \mathbf{X} has full column rank, for any $\beta, \beta^\dagger \in \mathbb{R}^{p \times J}$ there exist $\mathbf{z} \in \mathbb{R}^n$ and $\mathbf{z}^\dagger \in \mathbb{R}^n$ such that under model (14), $\log \mathbb{E}[\mathbf{Y} | \mathbf{X}, \beta, \mathbf{z}] = \log \mathbb{E}[\mathbf{Y} | \mathbf{X}, \beta^\dagger, \mathbf{z}^\dagger]$ if and only if $\beta^\dagger \in G_\beta$.

We prove Lemma 1 in Supporting Information Section 1. Lemma 1 demonstrates that while we cannot uniquely estimate β from data generated according to (14), we can estimate it up to the addition of constant terms to each of its rows. That is, while we cannot estimate differences across levels of covariate $X_{.k}$ in the log-means of \mathbf{W} given only data \mathbf{Y} , we *can* estimate relative differences in the log-mean of \mathbf{W} in category j_1 compared to in category j_2 . In microbiome sequencing studies, this represents a small loss of information because researchers typically aim to identify microbial taxa that show markedly different abundances across covariate groups of interest *when compared to the typical magnitude of these differences*. Therefore, estimating the equivalence class of β answers important scientific questions about microbial abundances.

We estimate the equivalence class of β by imposing identifiability constraints of the form $g(\beta_k) = 0$ on the rows β_k of β such that each G_β contains only a single unique element satisfying these constraints. Fitted means produced by our model are invariant to choice of constraint, but this choice does change the interpretation of elements of β . For example, under constraint $\beta_{kj} = 0$, $\beta_{kj'}$ represents $\log \mathbb{E}[W_{.j'} | X_{.k} = \mathbf{x}_{x_{k+1}}] - \log \mathbb{E}[W_{.j'} | X_{.k} = \mathbf{x}]$ minus the corresponding quantity for taxon j , where $\mathbf{x}_{x_{k+1}}$ is equal to \mathbf{x} in all elements excepting the k th, which is increased by 1 unit. We equivalently interpret $e^{\beta_{kj'}}$ as a fold-difference (multiplicative difference).

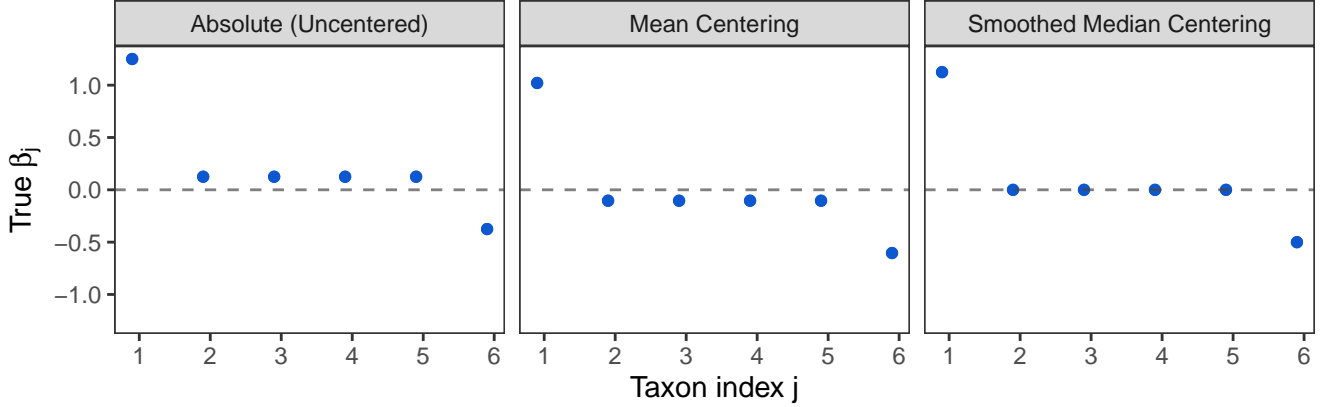


Figure 1: Because the mean function is only partially identifiable, true effect sizes β cannot be estimated on an “absolute” scale (left). Full identifiability is established via a constraint function, allowing us to estimate the log-fold differences in true abundances across groups relative to typical differences. The above illustrates the favorable qualities of centering via the pseudo-Huber smoothed median (right) compared to centering by the mean (middle). β_j for $j = 2, 3, 4, 5$ are unlikely to be of scientific interest (relative to $j = 1, 6$), and the smoothed median constrains these “uninteresting” taxa closer to zero than mean centering.

If we aim to compare log-mean differences across levels of a covariate to typical such differences across taxa, we might choose to impose identifiability by requiring $\text{median}_{j=1,\dots,J}(\beta_{kj}) = 0$. The robustness of the median is attractive: if few taxa exhibit large differences in mean concentration across levels of a covariate, this will in general minimally impact a median effect if most effects are small. By contrast, centering by a non-robust measure of location (e.g., mean) may result in unwanted behavior, because a single large effect β_{kj} will pull the mean away from the bulk of taxa (Figure 1). However, the median is not a differentiable function of β_k (its total derivative is not guaranteed to exist), which substantially complicates inference (see Section 4). Accordingly, we propose a smooth approximation to the median that shares its robustness properties, that is, the pseudo-Huber loss $g_p(\beta_k) = \arg \min_c \sum_{j=1}^J h_\delta(\beta_{kj} - c)$ for $h_\delta(x) = \delta^2 \left(\sqrt{1 + (x/\delta)^2} - 1 \right)$ for prespecified parameter $\delta > 0$ (Barron, 2019). The pseudo-Huber loss is approximately quadratic in a neighborhood of 0 and asymptotically approaches the function $|x|/\delta$ for large x . The parameter δ controls the size of the quadratic region around zero: as $\delta \downarrow 0$, $g_p(\beta_k)$ approaches the median, and as $\delta \rightarrow \infty$, it approaches the mean. We propose $\delta = 0.1$ as a reasonable default for many applications, though empirically we find that care is warranted when covariates are on very different scales. While we propose g_p as the default constrained function, any smooth g satisfying $g(\beta_k + \alpha) = g(\beta_k) + \alpha$ is reasonable, and the most appropriate constraint will depend on the scientific setting.

3 Estimation

3.1 Estimation under H_A

We estimate β (our target of inference) and \mathbf{z} (a nuisance parameter) using an estimating equations approach motivated by a Poisson likelihood with mean function (14). To address issues of infinite or undefined MLEs resulting from data separation, which commonly occurs in high-dimensional microbiome sequencing data (Bull et al., 2002), we introduce a Firth penalty on β derived from a formal equivalence between our model and the multinomial logistic model. We develop a fast algorithm to find the maximizer of the penalized likelihood by efficiently solving a sequence of score equations that converge to the score of the penalized likelihood within a neighbourhood of the global maximizer. As we will see in Sections 4 and 5, our estimator and accompanying hypothesis testing show excellent performance even when data has excess-Poisson variance, and even in small samples. All algorithms are provided as pseudocode in Supporting Information, and an R package implementing the method is available at [GitHub Link].

To motivate our estimator, we first introduce a Poisson log likelihood for our model. Letting β^j denote the j -th column of β and X_i denote the i -th row of \mathbf{X} , the Poisson log likelihood is

$$l^{\text{Poisson}}(\beta, \mathbf{z}) = \sum_{j=1}^J \left[\sum_{i=1}^n \left(Y_{ij}(X_i\beta^j + z_i) - \exp(X_i\beta^j + z_i) \right) \right]. \quad (6)$$

For fixed β , the maximizing value of \mathbf{z} is available in closed form

$$\hat{z}_i = \log \sum_{j=1}^J Y_{ij} - \log \sum_{j=1}^J \exp(X_i\beta^j), \quad (7)$$

and therefore we can profile out \mathbf{z} in likelihood (6) to give

$$l^{\text{profile}}(\beta) = \sum_{j=1}^J \left[\sum_{i=1}^n \left(Y_{ij} \log \frac{\exp(X_i\beta^j)}{\sum_{j'=1}^J \exp(X_i\beta^{j'})} - Y_{i\cdot} \frac{\exp(X_i\beta^j)}{\sum_{j'=1}^J \exp(X_i\beta^{j'})} \right) \right] + C \quad (8)$$

where C is constant (with respect to β) and $Y_{i\cdot} := \sum_{j=1}^J Y_{ij}$. Note that the profile likelihood (8) is equal to a multinomial log likelihood with a logistic link (up to a constant). This accords with both known results about the marginal Poisson distribution of multinomial random variables (Birch, 1963), and our observations on identifiability of β (only $p \times (J - 1)$ parameters can be identified in a multinomial logistic regression of a J -dimensional outcome on p regressors).

Unfortunately, the maximizer of l^{profile} will not be finite if there exists a perfect separating hyperplane (Albert and Anderson, 1984). To both guarantee the existence of an estimate and reduce its bias, we derive the Firth penalty associated with likelihood (8), observing the impact of the nuisance parameters \mathbf{z} on the correct bias-reducing penalty (Kosmidis and Firth, 2011). Fix $j^\dagger \in \{1, \dots, J\}$ and let $\tilde{\beta} := [\beta^{1^T}, \dots, \beta^{j^\dagger-1^T}, \beta^{j^\dagger+1^T}, \dots, \beta^{J^T}]^T$, that is, a column vector

containing stacked columns of β but with β^{j^\dagger} omitted. Let $\tilde{\mathbf{X}}_i = I_j^{[-j^\dagger]} \otimes X_i$, where $I_j^{[-j^\dagger]}$ indicates a $J \times J$ identity matrix whose j^\dagger -th column has been removed and \otimes is the Kronecker product, so $\tilde{\mathbf{X}}_i \in \mathbb{R}^{J \times p(J-1)}$ and $\tilde{\mathbf{X}} := [\tilde{\mathbf{X}}_1^T, \dots, \tilde{\mathbf{X}}_n^T]^T \in \mathbb{R}^{nJ \times p(J-1)}$. Define the fitted values $p_i = \exp(\tilde{\mathbf{X}}_i \tilde{\beta}) / \mathbf{1}_J^T \exp(\tilde{\mathbf{X}}_i \tilde{\beta}) \in \mathbb{R}^J$. We can then show that the information matrix associated with (8) is $\tilde{\mathbf{X}}^T \mathbf{V} \tilde{\mathbf{X}}$ where \mathbf{V} is a block diagonal matrix with i -th $J \times J$ block equal to $Y_i \cdot (\text{diag}(\mathbf{p}_i) - \mathbf{p}_i \mathbf{p}_i^T)$ with $\text{diag}(\mathbf{p}_i)$ indicating a diagonal matrix with diagonal elements equal to p_{i1}, \dots, p_{iJ} . Finally, we can express the Firth penalized multinomial log likelihood as follows:

$$l^{\text{penalized}} = l^{\text{profile}} + \frac{1}{2} \log |\tilde{\mathbf{X}}^T \mathbf{V} \tilde{\mathbf{X}}|, \quad (9)$$

where the penalty term depends on β through \mathbf{V} .

Remarkably, the penalized likelihood (9) is invariant to the choice of j^\dagger . This is because the Firth penalty is invariant under smooth reparametrizations for full exponential family models such as the multinomial distribution (Jeffreys, 1946; Firth, 1993), and the above parameterization implies the constraint $g(\beta_k) = \beta_{kj^\dagger} = 0$. Thus, we can estimate β under the ‘‘convenience constraint’’ $\beta_{kj^\dagger} = 0$ and impose the desired identifiability constraint post-hoc by subtracting the relevant $g(\tilde{\beta}_k)$ from each element of $\tilde{\beta}$. In practice we find that choosing j^\dagger to maximize $\sum_i \mathbf{1}_{[Y_{ij^\dagger} > 0]}$ improves the speed of optimization.

To find $\arg \max_{\tilde{\beta}} l^{\text{penalized}}$, we apply the iterative maximum likelihood algorithm of Kosmidis and Firth (2011), which maximizes (9) by iteratively solving multinomial score equations in augmented data $\mathbf{Y}^{(t)}$. Specifically, $Y_{ij}^{(t)} = Y_{ij} + h_{ij}/2$ where h_{ij} is the $(i-1) \times J + j$ -th diagonal element of the Poisson ‘‘hat’’ matrix $\mathbf{V}_p^{1/2} \tilde{\mathbf{G}} (\tilde{\mathbf{G}}^T \mathbf{V}_p \tilde{\mathbf{G}})^{-1} \tilde{\mathbf{G}}^T \mathbf{V}_p^{1/2}$ evaluated at current values of $\beta^{(t)}$ for \mathbf{V}_p an $nJ \times nJ$ diagonal matrix with $(i-1) \times J + j$ -th diagonal element equal to $\exp(X_i \beta^j + z_i)$ and $\tilde{\mathbf{G}} = [\tilde{\mathbf{X}} : \mathbf{I}_n \otimes \mathbf{1}_J] \in \mathbb{R}^{nJ \times (p(J-1)+n)}$ (i.e., the expanded design matrix for β , $\tilde{\mathbf{X}}$, side by side with a design matrix for \mathbf{z} , $\mathbf{I}_n \otimes \mathbf{1}_J$). We compute data augmentations under the restriction on z that $\sum_j \exp(X_i \beta^j + z_i) = Y_i$ by applying (7). Each iteration t of this algorithm is separable in $z, \beta^1, \dots, \beta^J$, and we therefore solve each iteration using coordinate descent, applying (7) to update z and updating each β^j with Fisher scoring followed by a line search. When a desired convergence threshold is reached, we impose the desired identifiability constraint by centering by $g(\tilde{\beta}_k^{(t_{\max})})$ as described previously.

3.2 Estimation under H_0

In Section 4, we present a robust score test for $\beta_{k^*j^*} = 0$ under constraint $g(\beta_{k^*}) = 0$, which requires fitting a model under the restriction $\beta_{k^*j^*} = g(\beta_{k^*})$. We therefore develop an augmented Lagrangian algorithm (Nocedal and Wright, 2006, p. 514) to solve this constrained optimization problem. The augmented Lagrangian function is

$$\mathcal{L}(\beta, z; \rho, u) := -l^{\text{Poisson}}(\beta, z; \mathbf{Y}^{(t_{\max})}) + u [g(\beta_{k^*}) - \beta_{k^*j^*}] + \frac{\rho}{2} [g(\beta_{k^*}) - \beta_{k^*j^*}]^2 \quad (10)$$

for $\mathbf{Y}^{(t_{\max})}$ from our model fit under H_A . For sequences $\rho^{(t)}$ and $u^{(t)}$ described below, we iteratively find maximizers $(\hat{\beta}_{\text{aug}}^{(t)}, \hat{z}_{\text{aug}}^{(t)})$ of (10) until $\hat{\beta}_{\text{aug}}^{(t)}$ satisfies the constraint $\beta_{k^*j^*} = g(\beta_{k^*})$ to

within a prespecified tolerance. While ideally (10) would be a function of $l^{\text{penalized}}(\beta; \mathbf{Y})$ instead of $l^{\text{Poisson}}(\beta, z; \mathbf{Y}^{(t_{\max})})$, updating data augmentations within Lagrangian steps adds an additional inner loop, and furthermore $l^{\text{Poisson}}(\beta, z; \mathbf{Y}^{(t_{\max})})$ is both a good approximation to $l^{\text{penalized}}(\beta; \mathbf{Y})$ and asymptotically equivalent under H_0 .

The presence of $g(\beta_{k^*})$ in (10) complicates optimization, as this term depends on an entire row of β . As a result, updating β column by column (as when fitting models under H_A) often results in slow convergence under H_0 . Hence, we instead minimize (10) via coordinate descent alternating between *block* updates to β via an approximate Newton step and updates to z via equation (7).

For fixed z , the augmented Lagrangian (10) has second derivative in $\tilde{\beta}$ (the vectorization of β with convenience constraint $\beta^{j^\dagger} = \mathbf{0}$) given by

$$\nabla^2 \mathcal{L} = -\nabla^2 l^{\text{Poisson}} + [u + \rho(g - \beta_{k^*j^*})] \nabla^2 g + \rho(\nabla g - \vec{e}_{[k^*j^*]})(\nabla g - \vec{e}_{[k^*j^*]})^T \quad (11)$$

where $\vec{e}_{[k^*j^*]}$ is a vector equal to 1 in the position in $\tilde{\beta}$ corresponding to $\beta_{k^*j^*}$ and zero elsewhere. $\nabla^2 l^{\text{Poisson}}$ is block diagonal and hence inexpensive to invert, and $\rho(\nabla g - \vec{e}_{[k^*j^*]})(\nabla g - \vec{e}_{[k^*j^*]})^T$ is a matrix of rank one. We therefore approximate the Hessian of (10) as $-\nabla^2 l + \rho(\nabla g - \vec{e}_{[k^*j^*]})(\nabla^T g - \vec{e}_{[k^*j^*]})$, and compute its inverse as a rank-one update to $-(\nabla^2 l)^{-1}$ via the Sherman-Morrison identity (Sherman and Morrison, 1950). For additional details, see Supporting Information Section 3.3.

In each iteration of the outer loop of our algorithm, we update ρ and u and obtain an approximate solution to (10). The update to u is given by $u^{(t+1)} = \rho^{(t)}[g(\beta_{k^*}^{(t)}) - \beta_{k^*j^*}^{(t)}]$. We update ρ if we have not progressed sufficiently toward a feasible solution in the past step: if $|g(\beta_{k^*}^{(t)}) - \beta_{k^*j^*}^{(t)}| > \kappa |g(\beta_{k^*}^{(t-1)}) - \beta_{k^*j^*}^{(t-1)}|$, we set $\rho^{(t+1)} = \tau \rho^{(t)}$ for $\kappa \in (0, 1)$ and $\tau > 1$; otherwise, we let $\rho^{(t+1)} = \rho^{(t)}$. We find that default values $\kappa = 0.8$ and $\tau = 2$ yield stable optimization in a broad range of settings. Lower κ and higher τ yield potentially faster optimization but at the cost of stability. In particular, if ρ grows too large, the augmented Lagrangian subproblem may become ill-conditioned.

We evaluate convergence with two criteria. Firstly, we require (primal) feasibility be satisfied to within a chosen tolerance: $|g(\beta_{k^*}) - \beta_{k^*j^*}| < \varepsilon$ for a small $\varepsilon > 0$. We additionally require that $\max_{k,j} |\beta_{kj}^{(t)} - \beta_{kj}^{(t-1)}| < \Delta$ for a small $\Delta > 0$.

4 Inference

We now discuss evaluating evidence for a difference in $\mathbb{E}W_j$ across levels of a covariate X_k , holding other covariates fixed. We explore the simple but common setting of testing $\overset{\circ}{H}_0 : \beta_{kj} = 0$, but the approach can be generalized to test more general hypotheses of the form $\mathbf{A}\beta = \mathbf{C}$ for fixed matrices $\mathbf{A} \in \mathbb{R}^{h \times p}$ and $\mathbf{C} \in \mathbb{R}^{h \times J}$. We are not able to test $\overset{\circ}{H}_0$ directly, as β is not fully identified. However, we are able to test $H_0^{(g)} : \beta_{kj} = g(\beta_k)$, or equivalently

$$\begin{aligned} H_0 : \quad & \log \mathbb{E}[W_j | X_k = x_k, X_{-k} = x_{-k}] - \log \mathbb{E}[W_j | X_k = x_k + 1, X_{-k} = x_{-k}] \\ & = g(\log \mathbb{E}[W | X_k = x_k, X_{-k} = x_{-k}] - \log \mathbb{E}[W | X_k = x_k + 1, X_{-k} = x_{-k}]) \end{aligned}$$

Thus, the interpretation of the test depends on the identifiability constraint. For example, we may test that a log-fold difference equals the smoothed median of such differences via $g(\beta_k) = g_p(\beta_k)$, or that a log-fold difference equals the log-fold difference of category 1 via $g(\beta_k) = \beta_{k1}$.

To construct a test of $H_0^{(g)}$, we restate $H_0^{(g)}$ as follows: $H_0^{(g)} : h(\beta) = 0$ with $h(\beta) = \beta_{kj} - g(\beta_k)$. We test nulls of this form via a robust score test, using the test statistic given in White (1982):

$$T_{RS} = S_{H_0}^T I_{H_0}^{-1} F_{H_0}^T (F_{H_0} I_{H_0}^{-1} D_{H_0} I_{H_0}^{-1} F_{H_0}^T)^{-1} F_{H_0} I_{H_0}^{-1} S_{F_{H_0}} \quad (12)$$

where S_{H_0} is the score evaluated at the maximum likelihood estimate $\hat{\beta}_0$ under the null, I_{H_0} is a consistent estimate of the information matrix under the null, F_{H_0} is given by $\frac{\partial h}{\partial \beta^T}$ evaluated at $\hat{\beta}_0$ and $D_{H_0} = \sum_{i=1}^n s_i(\hat{\beta}_0) s_i(\hat{\beta}_0)^T$ where $s_i(\beta) = \tilde{X}_i^T (Y_i - Y_i p_i(\beta))$ is the contribution to the score of Y_i . In practice, we use a score statistic T'_{RS} equal to $\frac{n}{n-1} T_{RS}$, where the term in front of T_{RS} is an adjustment due to Guo et al. (2005) that reduces the small-sample conservatism of the test. Under H_0 , T'_{RS} is asymptotically χ^2 -distributed with one degree of freedom; empirically, we observe that this test provides error rate control in large samples and conservative inference in small to moderate samples (Section 5). We also consider a robust Wald approach to testing hypotheses of the form $H_0^{(g)} : h(\beta) = 0$. The robust Wald statistic is given by

$$T_{RW} = h(\beta)^T (F_{H_A}^T I_{H_A} D_{H_A}^{-1} I_{H_A} F_{H_A})^{-1} h(\beta) \quad (13)$$

where F_{H_A} , I_{H_A} , and D_{H_A} are as above but evaluated under the full model. Since robust Wald testing does not require refitting a model under a null hypothesis, it offers a computational advantage over robust score testing. However, as explored in Section 5, robust Wald tests fail to adequately control Type 1 error in small samples.

5 Simulations

We conduct a small simulation study to examine the Type 1 error and power of our proposed tests. We simulate in two distributional settings: a correctly specified setting in which counts are independently Poisson-distributed, and a misspecified setting in which the mean model is correctly specified but counts follow independent zero-inflated negative binomial (ZINB) distributions. To obtain draws from a ZINB distribution, we first draw from a Negative Binomial distribution with mean μ given by our model and dispersion parameter $\phi = 5$ (thus, their variance is $\mu + \mu^2/\phi$). We multiply this draw with an independent Bernoulli draw ξ with $Pr(\xi = 1) = 0.4$ to obtain our final ZINB draw.

In all simulations, we simulate observations in two groups of equal size and test nulls of the form $\beta_{2j} - g_p(\beta_2) = 0$, where β_2 corresponds to between-group differences in log mean (up to a constant shift). The pseudo-Huber smoothing parameter for g_p is 0.1 in all simulations. The first row of β is fixed so that its odd elements form an linearly increasing sequence from -3 to 3 and its even elements form a similarly decreasing sequence from 3 to -3. We construct the first row of

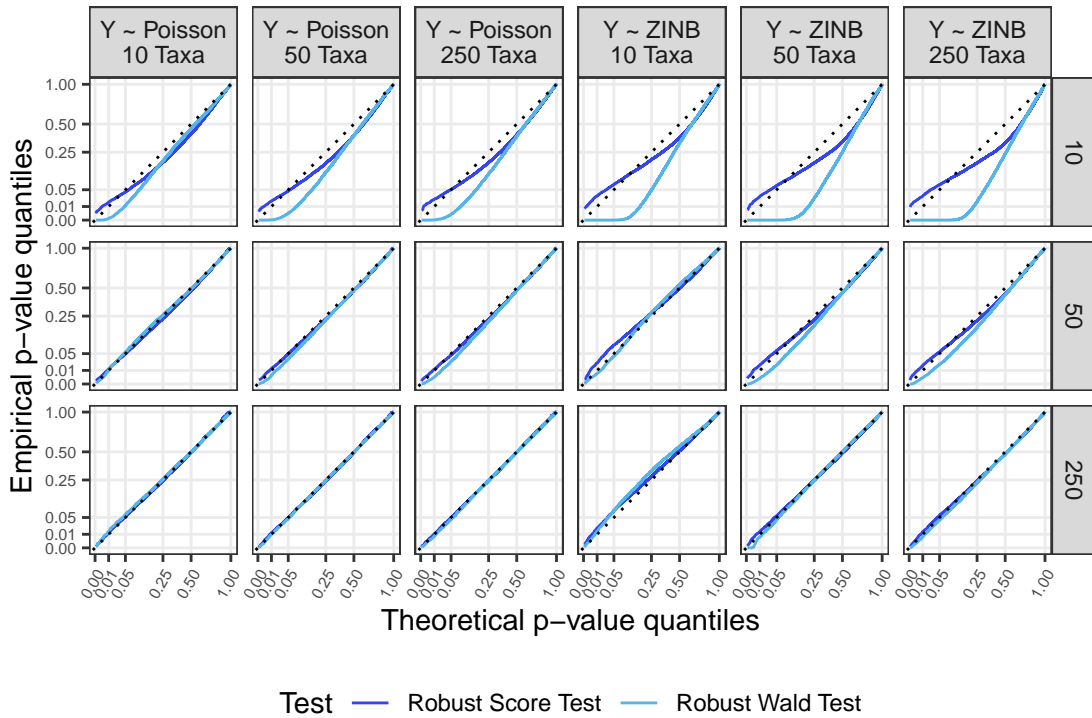


Figure 2: Q-Q plots comparing empirical quantiles (y-axis) of the robust score (dark blue) and robust Wald (light blue) p-values to theoretical quantiles (x-axis). A conservative test will produce a curve above the line $x = y$ for small p-values and an anti-conservative test will produce a curve below it. To aid in comparison of lower quantiles, both axes are presented on a square-root scale. 10,000 simulations were performed.

β in this way so that it is not strongly correlated with the second row of β . In null simulations, the second row of β , save its $J/2$ - and $(J+1)/2$ -th elements, which we set equal to zero, is given by $5 \times \sinh(x)/\sinh(10)$ where x consists of linearly increasing sequence from -10 to 10 , and \sinh indicates the hyperbolic sine function. Under alternatives, the second row of β is the same as just described with the exception of its $J/2$ -th element, which is set equal to 1 (under the “weak alternative”) or 5 (under the “strong alternative”). The values of β common to all three hypotheses were chosen to reflect a setting in which most taxa vary similarly in mean concentration across two groups, with a few taxa deviating from this typical variation. The values of $\beta_{k^*j^*}$ (i.e., the element of β for which we test equality to $g(\beta_{k^*})$) chosen for “weak” and “strong” alternatives are intended to reflect a modest (≈ 3 -fold deviation from typical ratio of mean concentrations across groups) effect that in some settings might nonetheless be of scientific interest, as well as a strong (≈ 150 -fold deviation from typical) effect. We simulate with total number of taxa $J \in \{10, 50, 25\}$ and total sample size $n \in \{10, 50, 250\}$. Note that total sample size indicates count of independent observations across both groups, so $n = 10$ corresponds to 5 observations in each of the two groups.

Figures 2 and 3 summarize the results of our simulations under the null and alternatives, respectively, with tabular results in Supporting Information Section 4. As expected, the robust score test exhibits conservatism in simulations under the null, with greater conservatism at smaller sample sizes and with ZINB-distributed counts. By contrast, the robust Wald test is anti-conservative in the smallest samples, with empirical Type 1 error 0.307 in ZINB simulations and 0.167 in Poisson simulations with $n = 10$, $J = 250$. In these two simulation settings, robust score tests have empirical Type 1 error 0.025 and 0.048, respectively. Notably, while the robust Wald test tends toward greater anti-conservatism when counts are not Poisson distributed, the robust score test appears to tend toward greater conservatism. At the highest sample size we considered, $n = 250$, empirical Type 1 error is close to nominal regardless of distribution, number of taxa, or test.

In simulations under the alternative, we observe higher power when counts are drawn from a Poisson than from a ZINB distribution, and when sample size is larger. While the robust Wald test exhibits higher power than the robust score test at smaller sample sizes, it also fails to control Type 1 error, so we nonetheless do not recommend this test for use in small or moderate samples. We also observe a modest impact of total number of taxa J on power: for ZINB simulations, we observe nondecreasing power in J . However, power of the score test does appear to decrease in J for Poisson simulations with $n = 10$.

6 Data analysis: Colorectal cancer microbial metaanalysis

In this section we consider a shotgun metagenomic dataset published by Wirbel et al. (2019). This dataset comprises a meta-analysis of five studies, each targeting possible associations between the composition of the human gut microbiome and colorectal cancer (CRC) risk. In each study, fecal samples were taken from participants with colorectal cancer as well as from healthy controls. We are interested in identifying microbial strains unusually enriched or depleted in study participants

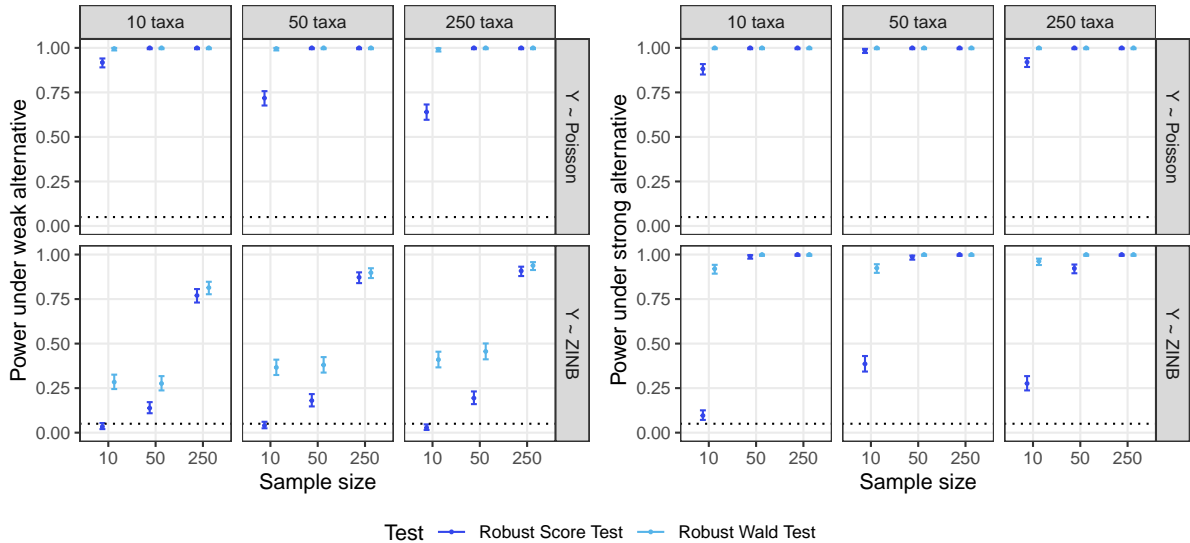


Figure 3: Empirical power to reject H_0 at the 5% level, estimated from 500 simulations. The panels at left show power to detect a smaller effect (≈ 3 -fold ratio of mean concentrations), and the panels at right show power to detect a larger effect (≈ 150 -fold ratio of mean concentrations). See Supporting Information Figure 1 for power curves.

with colorectal cancer as compared to otherwise similar control participants.

Each observation $Y_{ij} \in \mathbb{R}_{\geq 0}$ reflects the observed abundance of microbial strain j in fecal material of study participant i , measured as the depth of coverage of marker genes calculated by the mOTU profiler v2 (Milanese et al., 2019). We consider the “ideal” but unobserved data W_{ij} to be the cell concentration of strains in the stool of study participants. Participant data was pooled from five studies, yielding 575 study participants among whom 2342 unique strains were detected. In addition to metagenomic data, Wirbel et al. (2019) published clinical and demographic metadata including colorectal cancer status, age in years, binary gender, BMI, and timing of sampling relative to colonoscopy (sample taken prior to or following colonoscopy). Wirbel et al. (2019) applied stringent filtering criteria to remove low-abundance strains from their dataset. While not necessary for our methodology, to enable the comparison of our results with theirs, we applied the same filtering criterion, excluding all mOTUs that failed to exceed empirical relative abundances of 10^{-3} in at least three studies. We excluded 9 participants with missing covariate data (8 for BMI and 1 for timing of sampling relative to colonoscopy). With these exclusions, we analyze $n = 566$ study participants and $J = 845$ metagenomic strains.

We fit our proposed model to the untransformed mOTU data of Wirbel et al. (2019), applying Firth penalization as well as a smoothed median identifiability constraint to the rows of β . We include, in addition to an intercept and a term for CRC status (1 for CRC and 0 otherwise), terms in our model for age (linear spline with a single knot at median age 64 years), BMI (linear

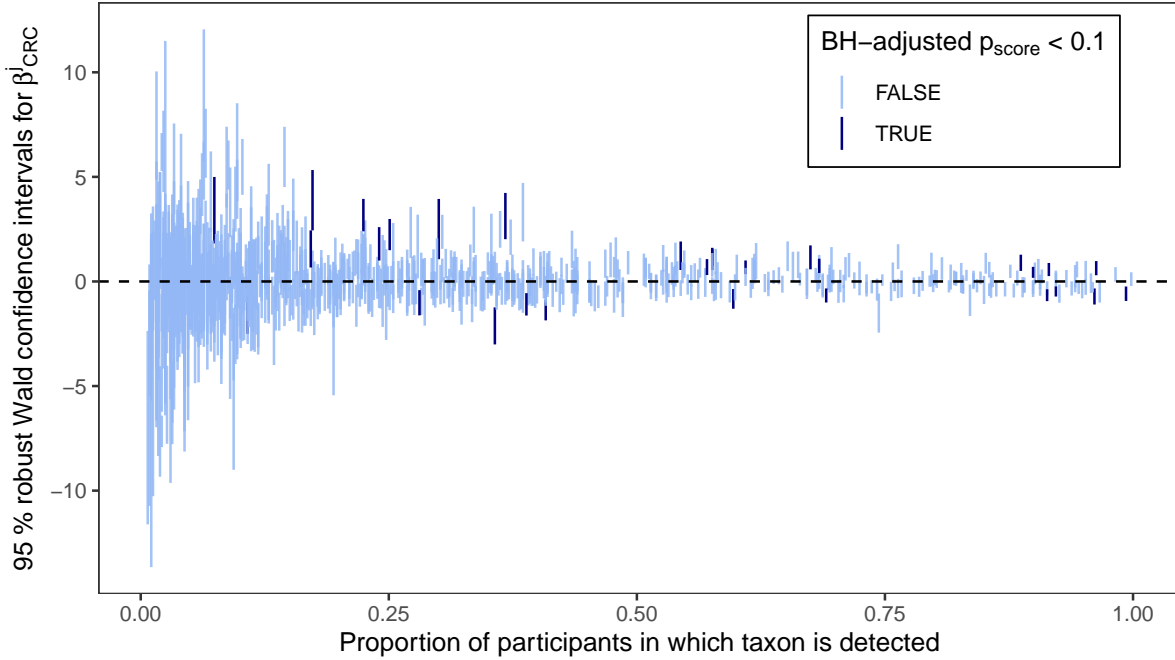


Figure 4: 95% Wald confidence intervals for taxon-specific CRC status effects estimated in our multivariable model (y-axis), plotted against the proportion of participants in all studies in which each taxon was detected (x-axis). Taxa with Benjamini-Hochberg-adjusted robust score p-values below 0.1 are shown in dark blue, with all others shown in light blue. Significantly differentially abundant taxa are identified across levels of observed prevalence.

spline with a single knot at median BMI 24.7 kg/m²), gender (1 for Male and 0 otherwise), study (4 indicator variables denoting the US, CN, DE and AT studies; we take FR to be the reference study), and whether fecal samples were taken after colonoscopy (1 if after, 0 if prior). Thus, coefficients on CRC status estimate the difference in log mean cell concentration comparing CRC patients to non-CRC controls who are alike in gender, BMI, age, study, and timing of stool sampling relative to colonoscopy, relative to typical such differences across taxa. We perform robust score tests and control the false discovery rate (using the Benjamini and Hochberg (1995) (BH) procedure, following Wirbel et al. (2019)) at 0.1.

Robust Wald confidence intervals for the coefficients on CRC status are shown in Figure 4. We identify 30 taxa for which we reject the null hypothesis of equal log mean cell concentration for CRC patients and (otherwise alike) non-CRC controls at a false discovery rate of 0.1 based on the robust score test. These taxa are denoted by navy-colored confidence intervals. Taxa are ordered along the x-axis by the proportion of participants in which they are detected, highlighting that significantly differentially abundant taxa are identified across the spectrum of detection levels. Taxa our analysis identifies as more enriched than typical among CRC patients relative to similar controls include an unknown *Dialister* species estimated to have ratio of mean cell concentration

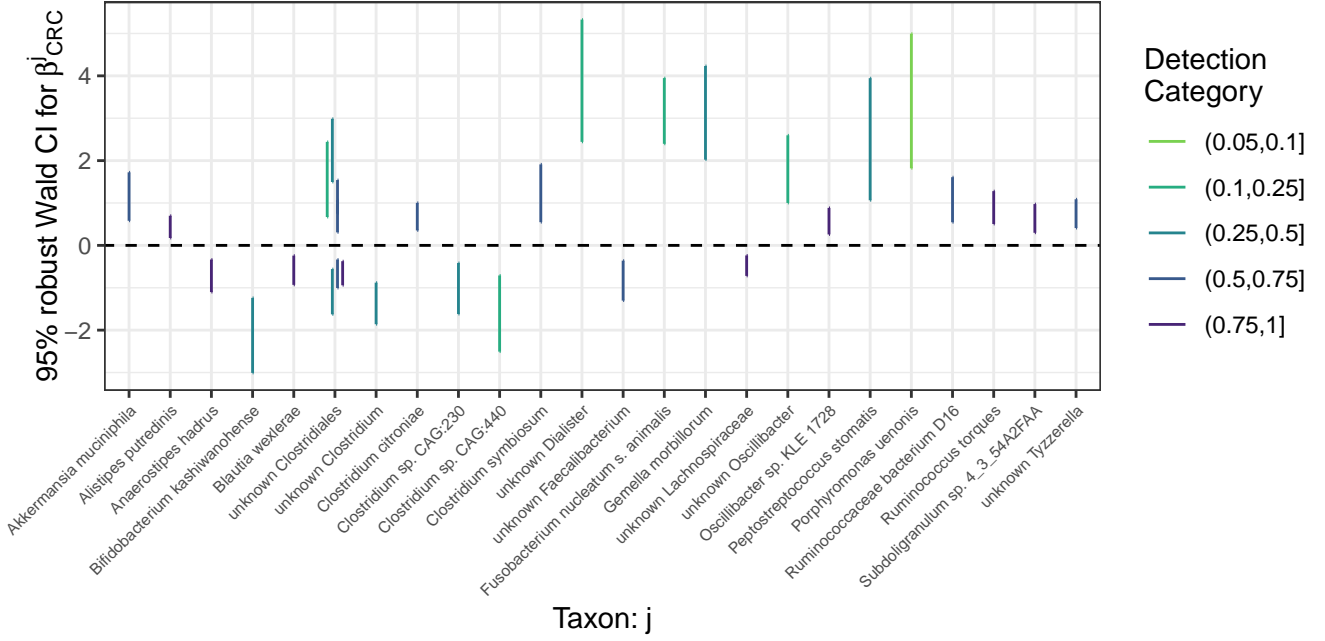


Figure 5: Taxa associated with CRC status in adjusted model at FDR level 0.1. Species designations are given on the x-axis; multiple confidence intervals are reported for unknown Clostridiales as multiple mOTUs with no known species designation were identified as significantly associated with CRC status in this class. 95% Wald confidence intervals for effect estimates (taxon-specific difference from smoothed median difference in log mean cell concentrations comparing CRC patients to controls, all other covariates held constant) are shown on the y-axis, with color indicating proportion of study participants in whom a given taxon was detected.

49 times greater than typical (95% CI 12 – 210; $p = 1.1 \times 10^{-6}$), *Porphyromonas uenonis* (30 times greater; 95% CI 6.2 – 150; $p = 0.0025$), *Fusobacterium nucleatum s. animalis* (24 times greater; 95% CI 11 – 52; $p = 2.2 \times 10^{-5}$), and *Gemella morbillorum* (23 times greater; 95% CI 7.6 – 69; $p = 0.0016$). Confidence intervals for all effect sizes that are significantly associated with CRC status at FDR cutoff 0.1 are given in Figure S7.

We identify a number of taxa associated with CRC status that are detected in relatively high proportion in the study populations. For example, we estimate for *B. kashiwanohense*, which was detected in 35.7% of study participants, that the ratio of mean stool cell concentrations for this taxon comparing CRC patients to alike controls is 8.6 times lower (95% CI 3.6 – 20.9; unadjusted robust score $p = 0.0022$) than the typical such ratio among taxa included in our analysis. This is consistent with a possible protective effect of *B. kashiwanohense*, but we cannot rule out association due to unmeasured confounding (e.g., through diet) or reverse causation (development of CRC induces relative depletion of *B. kashiwanohense*). We note that *B. kashiwanohense* was not identified as a taxon negatively associated with CRC status in the analysis of Wirbel et al. (2019).

We compare our results to those of Wirbel et al. (2019), as well as to 5 other popular differential abundance methods in the microbiome literature, in Figure 6. All panels show robust score p-values obtained from our adjusted model on the x-axis, and p-values obtained from comparator methods on the y-axis. We briefly describe details for each method here; please see Code Appendix for a reproducible workflow. (Top left) corncob (Martin et al., 2020) likelihood ratio test p-values with design matrix as for the proposed method and timing of sampling and study as dispersion covariates; (top center) ALDEx2 (Fernandes et al., 2014) with centered log-ratio transform and design matrix as for the proposed method and 512 Monte Carlo iterations; (top right) DESeq2 (Love et al., 2014) likelihood ratio test with design matrix as for the proposed method and “local” estimation of dispersions; (lower left) IFAA (Li et al., 2021) with design matrix as for the proposed method; (lower center) ANCOM-BC2 (Lin and Peddada, 2020) with design matrix as for the proposed method and without prevalence filtering; and (lower right) the results of Wirbel et al. (2019), who report a blocked Wilcoxon test performed on proportion-scale mOTU data, with blocking on study and timing of sampling relative to colonoscopy (five p-values of zero are altered to 10^{-25} for visual comparison). While all methods target slightly different estimands, our proposed methodology is most similar to the ALDEx2 and ANCOM-BC2 target estimands, which is consistent with the relatively high sample Spearman correlation of p-values between our method when compared with ALDEx2 (0.53) and ANCOM-BC2 (0.65).

Finally, we contrast our results with those of Wirbel et al. (2019), finding substantial variation in the ordering of p-values between our proposed method and the blocked Wilcoxon test (Spearman correlation 0.44). Only 45 of the 94 taxa Wirbel et al. (2019) identified as significantly associated with CRC status are among the 94 taxa most significantly associated with CRC status in our analysis, and of the 30 taxa we highlight at FDR level 0.1, only 10 are among the 30 most highly significant taxa identified by Wirbel et al. (2019). We believe that this lack of concordance is likely due to two major factors. Firstly, our model adjusts for a larger set of potential confounders than do Wirbel et al. (2019), which may account for our discrepant findings. In addition, we estimate effects on the scale of log mean cell concentration, whereas Wirbel et al. (2019) conduct tests on the read proportion scale. Because a perturbation to the abundance of a small number of taxa on the cell concentration scale induces a dense perturbation on the proportion scale, analyses on the proportion scale may highlight taxa that do not vary in a scientifically interesting way on the cell concentration scale. Similarly, analyses performed on proportion data may fail to detect scientifically meaningful effects on the cell concentration scale because of fluctuations in cell concentration among other taxa.

7 Discussion

In this paper we present a regression method for inference on means of a nonnegative multivariate outcome W observed after perturbation by unknown sample-specific scaling terms z and category-specific detection effects δ . Our method is motivated by microbiome sequencing experiments, in

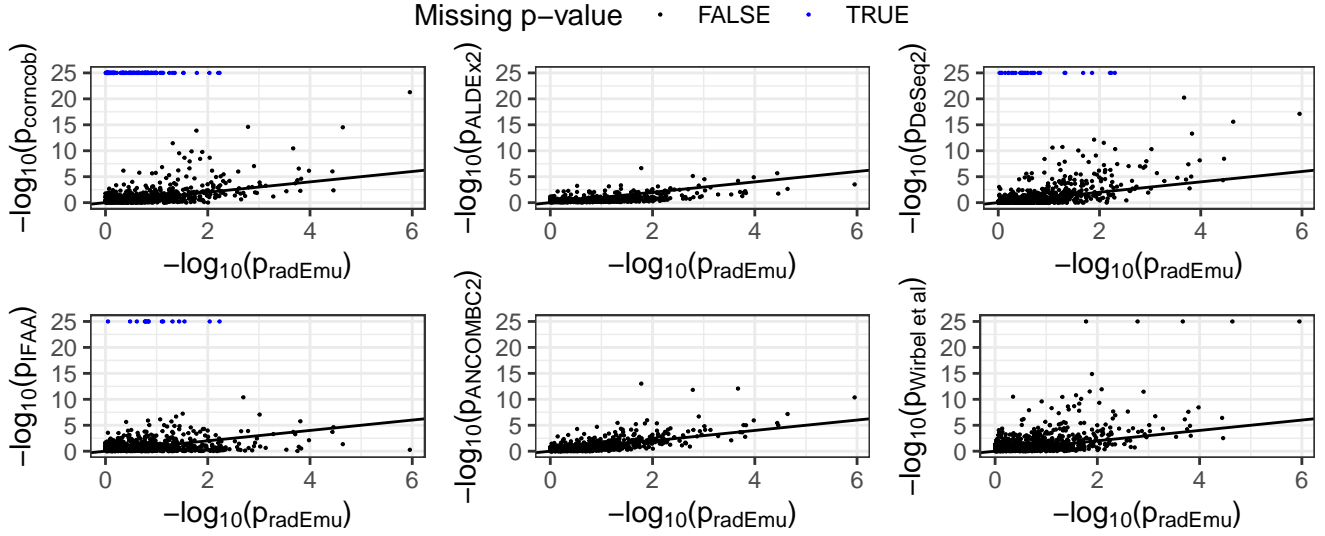


Figure 6: Negative \log_{10} p-values from distinct approaches to differential abundance analyses based on the Wirbel et al. (2019) dataset. The proposed method's robust score test p-values are shown on the x-axis, and comparator methods on the y-axis. The proposed method produces smaller p-values in 45%, 68%, 52%, 49%, 51% and 41% of cases for corncob, ALDEX2, DESeq2, IFAA, ANCOM-BC2 and blocked Wilcoxon respectively, with rank correlations of 0.45, 0.53, 0.57, 0.14, 0.65 and 0.44. Wirbel et al. (2019) report some p-values equal to zero; to allow graphing on the log scale, we replace these values with 10^{-25} . In addition to the missing/uncomputable p-values of corncob, DESeq2 and IFAA, two DESeq2 were so small as to make plotting infeasible; these observations correspond to $(p_{\text{radEmu}}, p_{\text{DESeq2}})$ tuples of $(10^{-1.8}, 10^{-31})$ and $(10^{-2.8}, 10^{-33})$.

which outcomes of interest (microbial cell concentration across many species) are typically observed indirectly via sequencing, which is known to be subject to both sample-specific scaling and taxon-specific distortion (McLaren et al., 2019). However, we anticipate that our method may find application in other settings; in particular, we expect that it may be appropriate for analysis of various types of 'omics measurements, where similar scaling and detection effects are likely to distort measurements.

Our method has a number of advantages over existing methods commonly applied to perform differential abundance analyses in microbiome studies. Firstly, it targets a population estimand that is distinguishable from sample- and category-scaling effects and that exists under realistic conditions (positivity of population mean abundances $\mathbb{E}W_j$). Notably, we do not require positivity of true sample abundances W_{ij} . Secondly, our method does not require data transformations, such as log-ratio transformations or relative abundance transformations. This allows us to use information regarding the precision of observations in estimation. It also avoids the ad-hoc fixes (e.g., adding a small pseudocount to zero observations, restricting attention to nonzero counts, or attempting to infer whether observed zeroes are due to insufficient read depth or reflect true absence of a taxon) that are necessary to apply log-ratio transformations to data containing zeroes. Additionally, we employ a model-robust score test that controls Type 1 error even in small samples with large excess-Poisson dispersion and high degrees of sparsity. Finally, we incorporate an identifiability constraint that may be flexibly specified to suit varying scientific settings. In particular, we do not require a choice of reference taxon. That said, if such a taxon is available, our method is able to take advantage of this information.

An additional consideration in practical applications for this method is measurement error. While our target estimand β can be estimated in the presence of systematic measurement error δ , no such guarantees exist for other kinds of measurement error, such as cross-sample contamination. Accordingly, we encourage the use of decontamination techniques (Davis et al., 2018; Clausen and Willis, 2022) prior to use of our proposed method.

Our method admits several possible extensions. In contexts where it is scientifically plausible that the parameter of interest β_k is sparse, enforcing sparsity via ℓ_1 penalization is an attractive option. However, we note that if most elements of β_k are truly equal to zero, β_k is correctly specified under pseudo-Huber constraints (up to negligible differences between medians and pseudo-Huber centers). In addition, while estimation will be valid in the presence of longitudinal or cluster-dependent observations, it remains to extend our inferential methods to this setting. Finally, it may be of interest to extend our method to address settings in which Neyman-Scott-type problems (Neyman and Scott, 1948) are of concern due to the presence of nuisance parameters whose dimension grows with number of observations.

Open-source software implementing the method (including long and short-form documentation) is available at github.com/statdivlab/radEmu. `radEmu` abbreviates `radEmuAbPill`, which denotes “using relative absolute data to estimate multiplicative differences in absolute abundances with partially identified log-linear models”.

References

- Albert, A. and Anderson, J.A. (1984). On the existence of maximum likelihood estimates in logistic regression models. *Biometrika* 71(1), 1–10.
- Barron, J.T. (2019). A general and adaptive robust loss function. In *Proceedings of the IEEE/CVF Conference on Computer Vision and Pattern Recognition*, pp. 4331–4339.
- Benjamini, Y. and Hochberg, Y. (1995). Controlling the false discovery rate: a practical and powerful approach to multiple testing. *Journal of the Royal Statistical Society: Series B* 57(1), 289–300.
- Birch, M. (1963). Maximum likelihood in three-way contingency tables. *Journal of the Royal Statistical Society Series B: Statistical Methodology* 25(1), 220–233.
- Bull, S.B., Mak, C. and Greenwood, C.M. (2002). A modified score function estimator for multinomial logistic regression in small samples. *Computational Statistics & Data Analysis* 39(1), 57–74.
- Clausen, D.S. and Willis, A.D. (2022). Modeling complex measurement error in microbiome experiments. *arXiv preprint arXiv:2204.12733*.
- Davis, N.M. et al (2018). Simple statistical identification and removal of contaminant sequences in marker-gene and metagenomics data. *Microbiome* 6(1), 1–14.
- Fernandes, A.D. et al (2014). Unifying the analysis of high-throughput sequencing datasets: characterizing rna-seq, 16s rrna gene sequencing and selective growth experiments by compositional data analysis. *Microbiome* 2(1), 1–13.
- Firth, D. (1993). Bias reduction of maximum likelihood estimates. *Biometrika* 80(1), 27–38.
- Guo, X. et al (2005). Small-sample performance of the robust score test and its modifications in generalized estimating equations. *Statistics in Medicine* 24(22), 3479–3495.
- Jeffreys, H. (1946). An invariant form for the prior probability in estimation problems. *Proceedings of the Royal Society of London. Series A. Mathematical and Physical Sciences* 186(1007), 453–461.
- Kaul, A. et al (2017). Analysis of microbiome data in the presence of excess zeros. *Frontiers in Microbiology* 8, 2114.
- Kosmidis, I. and Firth, D. (2011). Multinomial logit bias reduction via the poisson log-linear model. *Biometrika* 98(3), 755–759.

- Li, Z. et al (2021). Ifaa: robust association identification and inference for absolute abundance in microbiome analyses. *Journal of the American Statistical Association* 116(536), 1595–1608.
- Lin, H. and Peddada, S.D. (2020). Analysis of compositions of microbiomes with bias correction. *Nature Communications* 11(1), 3514.
- Love, M.I., Huber, W. and Anders, S. (2014). Moderated estimation of fold change and dispersion for rna-seq data with deseq2. *Genome Biology* 15(12), 1–21.
- Mandal, S. et al (2015). Analysis of composition of microbiomes: a novel method for studying microbial composition. *Microbial ecology in health and disease* 26(1), 27663.
- Martin, B.D., Witten, D. and Willis, A.D. (2020). Modeling microbial abundances and dysbiosis with beta-binomial regression. *The Annals of Applied Statistics* 14(1), 94.
- McLaren, M.R., Willis, A.D. and Callahan, B.J. (2019). Consistent and correctable bias in metagenomic sequencing experiments. *eLife* 8.
- Milanese, A. et al (2019). Microbial abundance, activity and population genomic profiling with motus2. *Nature Communications* 10(1), 1014.
- Moffatt, M.F. and Cookson, W.O. (2017). The lung microbiome in health and disease. *Clinical Medicine* 17(6), 525.
- Nearing, J.T. et al (2022). Microbiome differential abundance methods produce different results across 38 datasets. *Nature Communications* 13(1), 1–16.
- Neyman, J. and Scott, E.L. (1948). Consistent estimates based on partially consistent observations. *Econometrica: Journal of the Econometric Society*, 1–32.
- Nocedal, J. and Wright, S.J. (1999). *Numerical optimization*. Springer.
- Nocedal, J. and Wright, S.J. (2006). *Numerical optimization*. Springer.
- Paulson, J.N., Pop, M. and Bravo, H.C. (2013). metagenomeseq: Statistical analysis for sparse high-throughput sequencing. *Bioconductor package* 1(0), 191.
- Robinson, M.D., McCarthy, D.J. and Smyth, G.K. (2010). edgeR: a bioconductor package for differential expression analysis of digital gene expression data. *Bioinformatics* 26(1), 139–140.
- Segata, N. et al (2011). Metagenomic biomarker discovery and explanation. *Genome Biology* 12(6), 1–18.
- Sherman, J. and Morrison, W.J. (1950). Adjustment of an inverse matrix corresponding to a change in one element of a given matrix. *The Annals of Mathematical Statistics* 21(1), 124–127.

- Shreiner, A.B., Kao, J.Y. and Young, V.B. (2015). The gut microbiome in health and in disease. *Current Opinion in Gastroenterology* 31(1), 69.
- White, H. (1982). Maximum likelihood estimation of misspecified models. *Econometrica*, 1–25.
- Williamson, B.D., Hughes, J.P. and Willis, A.D. (2022). A multiview model for relative and absolute microbial abundances. *Biometrics* 78(3), 1181–1194.
- Wirbel, J. et al (2019). Meta-analysis of fecal metagenomes reveals global microbial signatures that are specific for colorectal cancer. *Nature Medicine* 25(4), 679–689.
- Yamashita, Y. and Takeshita, T. (2017). The oral microbiome and human health. *Journal of Oral Science* 59(2), 201–206.
- Young, V.B. (2017). The role of the microbiome in human health and disease: an introduction for clinicians. *BMJ* 356.

S1 Proof of Lemma 2.1

Lemma: For arbitrary $\beta^\dagger \in \mathbb{R}^{p \times J}$, define $G_{\beta^\dagger} = \{\beta \in \mathbb{R}^{p \times J} : \beta = \beta^\dagger + \alpha \mathbf{1}_J^T \text{ for some } \alpha \in \mathbb{R}^p\}$. If \mathbf{X} has full column rank, for any $\beta, \beta^* \in \mathbb{R}^{p \times J}$ there exist $\mathbf{z} \in \mathbb{R}^n$ and $\mathbf{z}^* \in \mathbb{R}^n$ such that under the model

$$\log \mathbb{E}[Y_i | X_i, \beta^*, z_i, \delta] = z_i \mathbf{1}_J^T + X_i \beta^* + \delta^T, \quad (14)$$

$\log \mathbb{E}[\mathbf{Y} | \mathbf{X}, \beta, \mathbf{z}] = \log \mathbb{E}[\mathbf{Y} | \mathbf{X}, \beta^*, \mathbf{z}^*]$ if and only if $\beta^* \in G_\beta$.

Proof. Suppose $\beta^* \in G_\beta$. Then there exists an $\alpha \in \mathbb{R}^p$ such that $\beta^* = \beta + \alpha \mathbf{1}_J^T$ and by ((2), main text), for any \mathbf{z} and $\mathbf{z}^* := \mathbf{z} + \mathbf{X}\alpha$, $\log \mathbb{E}[\mathbf{Y} | \mathbf{X}, \beta, \mathbf{z}] = \log \mathbb{E}[\mathbf{Y} | \mathbf{X}, \beta^*, \mathbf{z}^*]$. Now suppose $\beta^* \notin G_\beta$. If there exist \mathbf{z}, \mathbf{z}^* such that $\log \mathbb{E}[\mathbf{Y} | \mathbf{X}, \beta, \mathbf{z}] = \log \mathbb{E}[\mathbf{Y} | \mathbf{X}, \beta^*, \mathbf{z}^*]$, we have

$$\begin{aligned} \mathbf{z} \mathbf{1}_J^T + \mathbf{X}\beta &= \mathbf{z}^* \mathbf{1}_J^T + \mathbf{X}\beta^* \\ \Rightarrow \mathbf{X}(\beta - \beta^*) &= (\mathbf{z}^* - \mathbf{z}) \mathbf{1}_J^T \\ \Rightarrow \mathbf{X}^T \mathbf{X}(\beta - \beta^*) &= \mathbf{X}^T (\mathbf{z}^* - \mathbf{z}) \mathbf{1}_J^T \\ \Rightarrow (\beta - \beta^*) &= (\mathbf{X}^T \mathbf{X})^{-1} \mathbf{X}^T (\mathbf{z}^* - \mathbf{z}) \mathbf{1}_J^T \\ \Rightarrow \beta^* &= \beta + \tilde{\alpha} \mathbf{1}_J^T \text{ for } \tilde{\alpha} := (\mathbf{X}^T \mathbf{X})^{-1} \mathbf{X}^T (\mathbf{z}^* - \mathbf{z}) \in \mathbb{R}^p \\ \Rightarrow \beta^* &\in G_\beta \end{aligned}$$

which is a contradiction. Hence $\beta^* \notin G_\beta$ guarantees that for no \mathbf{z}, \mathbf{z}^* do we have $\log \mathbb{E}[\mathbf{Y} | \mathbf{X}, \beta, \mathbf{z}] = \log \mathbb{E}[\mathbf{Y} | \mathbf{X}, \beta^*, \mathbf{z}^*]$. \square

S2 Pseudo-Huber Centering

For a generic vector $x = [x_1, \dots, x_J] \in \mathbb{R}^J$ and smoothing parameter $\delta > 0$, we define the pseudo-Huber smoothed median c^* of x as follows:

$$c^* = \operatorname{argmin}_c \sum_j \delta^2 \left[1 + \left(\frac{x_j - c}{\delta} \right)^2 \right]^{1/2}$$

We now derive the form of $\frac{\partial}{\partial x_j} c^*$, which is needed for optimization and testing.

First, we have

$$\begin{aligned} & \frac{\partial}{\partial c} \left[\sum_j \delta^2 \left[1 + \left(\frac{x_j - c}{\delta} \right)^2 \right]^{1/2} \right] \Big|_{c=c^*} = 0 \\ \Rightarrow & \sum_j \frac{\delta^2}{2} \left[1 + \left(\frac{x_j - c}{\delta} \right)^2 \right]^{-1/2} 2 \left(\frac{x_j - c}{\delta} \right) \left(\frac{-1}{\delta} \right) = 0 \\ \Rightarrow & \sum_j w_j (x_j - c) = 0 \text{ for } w_j := \left[1 + \left(\frac{x_j - c}{\delta} \right)^2 \right]^{-1/2} \end{aligned}$$

We also have

$$\begin{aligned} \frac{\partial}{\partial x_{j^\dagger}} w_j &= -\frac{1}{2} \left[1 + \left(\frac{x_j - c}{\delta} \right)^2 \right]^{-3/2} 2 \left(\frac{x_j - c}{\delta} \right) \left(\frac{\mathbf{1}_{[j=j^\dagger]} - \frac{\partial}{\partial x_{j^\dagger}} c}{\delta} \right) \\ &= -w_j^3 \left(\frac{x_j - c}{\delta^2} \right) \left[\mathbf{1}_{[j=j^\dagger]} - \frac{\partial}{\partial x_{j^\dagger}} c \right] \end{aligned}$$

Before proceeding, we will derive a useful identity. Let $y := \frac{x_j - c}{\delta}$. Then we have

$$\begin{aligned} w_j - w_j^3 \left(\frac{x_j - c}{\delta} \right)^2 &= (1 + y^2)^{-1/2} - (1 + y^2)^{-3/2} y^2 \\ &= \frac{1}{(1 + y^2)^{1/2}} - \frac{y^2}{(1 + y^2)^{3/2}} \\ &= \frac{1 + y^2}{(1 + y^2)^{3/2}} - \frac{y^2}{(1 + y^2)^{3/2}} \\ &= \frac{1}{(1 + y^2)^{3/2}} \\ &= w_j^3 \end{aligned}$$

We can now use implicit differentiation to find $\frac{\partial}{\partial x_j} c^*$

$$\begin{aligned}
& \frac{\partial}{\partial x_j} \sum_j w_j (x_j - c^*) \\
&= \sum_j \left[w_j (\mathbf{1}_{[j=j^\dagger]} - \frac{\partial}{\partial x_{j^\dagger}} c^*) - w_j^3 \left(\frac{x_j - c^*}{\delta^2} \right) \left[\mathbf{1}_{[j=j^\dagger]} - \frac{\partial}{\partial x_{j^\dagger}} c^* \right] \right] = 0 \\
&\Rightarrow \sum_j \left[w_j - w_j^3 \left(\frac{x_j - c^*}{\delta} \right)^2 \right] \frac{\partial}{\partial x_{j^\dagger}} c^* = w_{j^\dagger} - w_{j^\dagger}^3 \left(\frac{x_{j^\dagger} - c^*}{\delta} \right)^2 \\
&\Rightarrow \sum_j w_j^3 \frac{\partial}{\partial x_{j^\dagger}} c^* = w_{j^\dagger}^3 \text{ by the identity above} \\
&\Rightarrow \frac{\partial}{\partial x_{j^\dagger}} c^* = \frac{w_{j^\dagger}^3}{\sum_j w_j^3}
\end{aligned}$$

For a given x , to find the pseudo-Huber center $c^*(x) = \arg \min_c \sum_j \delta^2 \left[1 + \left(\frac{x_j - c}{\delta} \right)^2 \right]^{1/2}$ with parameter δ by minimizing successive quadratic approximations to $f(c; x, \delta) := \sum_j \delta^2 \left[1 + \left(\frac{x_j - c}{\delta} \right)^2 \right]^{1/2}$. For current value $c^{(t)}$ of c , we compute, for $j = 1, \dots, J$, $w_j^{(t)} := \left[1 + \left(\frac{x_j - c^{(t)}}{\delta} \right)^2 \right]^{-1/2}$. Letting $h^{(t)}(c) = \sum_j \frac{1}{2} w_j^{(t)} \left(\frac{x_j - c}{\delta} \right)^2$, we then construct quadratic approximation $\tilde{f}^{(t)} := f(c^{(t)}) - h^{(t)}(c^{(t)}) + h^{(t)}(c)$ to f at $c^{(t)}$. We update $c^{(t+1)}$ as the minimizer of $\tilde{f}^{(t)}$, which is conveniently the weighted mean of x with weights $\frac{1}{\sum_j w_j} (w_1, \dots, w_J)$.

S3 Algorithms

S3.1 Unconstrained optimization

Algorithm 1 Coordinate Descent for Maximum Likelihood Estimation

1. Initiate with
 - Data (X, Y)
 - Starting value $\beta^{(0)}$ for β
 - Identifiability constraint $g(\beta_k) = 0$ for $k = 1, \dots, p$
 - Convergence tolerance $\epsilon > 0$
 - Iteration limit t_{\max}
 - Choice of working identifiability constraint $\beta^{j^\dagger} = 0$ (e.g., j^\dagger such that $\sum_i \mathbf{1}_{Y_{ij^\dagger} > 0}$ is maximized)
 2. For $k = 1, \dots, p$, impose working constraint by setting $\beta_k = \beta_k - \beta_{kj^\dagger}$
 3. For iteration $t = 1, \dots, t_{\max}$
 - (a) For $j \in \{1, \dots, J\} \setminus \{j^\dagger\}$, update β^j , the j -th column of β with single iteration of algorithm (2)
 - (b) Update z_i for $i = 1, \dots, n$ via equation (7).
 - (c) If $\max_{k,j} |\beta_{kj}^{(t)} - \beta_{kj}^{(t-1)}| < \epsilon$ or if $t = t_{\max}$
 - For $k = 1, \dots, p$ enforce original identifiability constraint by setting $\beta_k = \beta_k^{(t)} - g(\beta_k^{(t)})$.
 - Exit algorithm and return β .
 - (d) Otherwise increment t by 1 and return to step 3a.
-

Algorithm 2 Scoring Update with Line Search

1. Initiate with

- Data (X, Y^j)
- Current values of β^j and \mathbf{z}
- Maximum step size s

2. Then

(a) Compute

- gradient $S^j = X^T(Y^j - \boldsymbol{\mu}^j)$ for $\boldsymbol{\mu}^j = [\mu_1^j, \dots, \mu_n^j]^T = [\exp(X_1\beta^j + z_1), \dots, \exp(X_n\beta^j + z_n)]^T$
- information $I^j = X^T W X$ for W a diagonal matrix with i -th diagonal entry μ_i^j

(b) Compute update direction $d^j = I^{j-1} S^j$. If I^j is poorly conditioned, attempt to compute update direction as $(I^j + \sigma \mathbf{I})^{-1} S^j$, sequentially increasing σ until $(I^j + \sigma \mathbf{I})^{-1}$ is numerically invertible. (I^j is theoretically always full rank if X is full rank; in practice, it may be poorly conditioned numerically.)

(c) Perform line search to find update $\beta^j + \alpha d$ satisfying $l(\beta^j + \alpha d) \geq l(\beta^j) + c\alpha d^T \nabla l$ (i.e., the Armijo rule) where l is the log likelihood function evaluated in β^j with z held fixed, $c > 0$ is a constant (by default we use $c = 10^{-4}$ as suggested by Nocedal and Wright (1999, Ch. 17), ∇l is the partial derivative of the log likelihood with respect to β^j , and α is initiated at 0.5 and halved until the Armijo condition is met. After the Armijo condition is met, optionally rescale αd so that $\max_k |\alpha d_k| \leq \xi$ for some maximum step length ξ before accepting update $\beta^j + \alpha d$ to prevent large steps that may lead to ill conditioning. We by default use $\xi = 1$.

Algorithm 3 Penalized Likelihood Estimation via Iterative Maximum Likelihood

1. Initiate with
 - Data (X, Y)
 - Starting value $\beta^{(0)}$ for β
 - Identifiability constraint $g(\beta_k) = 0$ for $k = 1, \dots, p$
 - Convergence tolerance $\epsilon > 0$
 - Iteration limit t_{\max}
 2. Set $Y^{(1)} = \mathbf{Y} + \delta$ for some $\delta \geq 0$. (Choosing $\delta > 0$ is not necessary but can ameliorate slow convergence issues that otherwise might arise in the first iteration due to separation.)
 3. For iteration $t = 1, \dots, t_{\max}$
 - (a) Update $\beta^{(t)}$ using algorithm 2 applied to data $\mathbf{Y}^{(t)}$ with other arguments as specified above
 - (b) Update $\mathbf{Y}^{(t+1)}$ using $\beta^{(t)}$ and z as laid out in Section 3 of main text
 - (c) If $\max_{k,j} |\beta_{kj}^{(t)} - \beta_{kj}^{(t-1)}| < \epsilon$ or if $t = t_{\max}$, exit and return β . Otherwise increment t and return to step 3a.
-

S3.2 Constrained optimization

Algorithm 4 Constrained Estimation

1. Initiate with
 - Covariate matrix \mathbf{X}
 - Initial value of β and augmented outcomes $\tilde{\mathbf{Y}}$ obtained via fitting an unconstrained penalized model
 - Constraint function g
 - Row and column indexes k^*, j^* for the element of β to be constrained
 - Initial value of augmented Lagrangian penalty parameter ρ
 - Values $\kappa \in (0, 1)$ and $\tau > 1$ controlling scaling of ρ in each iteration
 - Convergence tolerance ϵ
 - Constraint tolerance γ
 - Iteration limits t_{max} for outer loop and t_{max}^{inner} for inner loop
 2. Set $u^{(1)} = \rho(\beta_{k^*j^*} - g(\beta_{k^*}))$ and $\rho^{(1)} = \rho$
 3. Then for iteration $t = 1, \dots, t_{max}$
 - (a) Define $\mathcal{L}^{(t)} = -l(\beta, z) + u^{(t)}[\beta_{k^*j^*} - g(\beta_{k^*})] + (\rho^{(t)}/2)[\beta_{k^*j^*} - g(\beta_{k^*})]^2$
 - (b) Via block coordinate descent in β and z , obtain $(\beta^{(t)}, z^{(t)})$ satisfying $\|\nabla \mathcal{L}^{(t)}\|_2 < \epsilon$
 - Coordinate descent steps in β are approximate Newton steps using $-\nabla^2 l + \rho \nabla g \nabla^T g$ as an approximation to the Hessian of the augmented Lagrangian
 - Coordinate descent steps in z are available in closed form
 - (c) If $R^{(t)} := \beta_{k^*j^*}^{(t)} - g(\beta_{k^*}^{(t)})$ satisfies $|R^{(t)}| < \gamma$ or $t = t_{max}$, exit and return $\beta^{(t)}$
 - (d) Otherwise, set $\rho^{(t+1)} = \tau \rho^{(t)}$ and $u^{(t+1)} = \rho^{(t+1)} R^{(t)}$
-

S3.3 Additional Details: Efficient approximate Newton method

As discussed in the main text (Section 3.2), we approximate the Hessian of the augmented Lagrangian induced by our constrained optimization problem as $-\nabla^2 l + \rho(\nabla g - \vec{e}_{[k^*j^*]})(\nabla^T g - \vec{e}_{[k^*j^*]})$ and compute its inverse as a rank-one update to $-(\nabla^2 l)^{-1}$ via the Sherman-Morrison identity.

We may justify this choice on several grounds. When ρ is small in early iterations of our algorithm, u will also be small, and so provided g is not too large (which in practice it is not), $-\nabla^2 l$ will well approximate $\nabla^2 \mathcal{L}$. In later iterations, we expect to have g close to zero and $\rho \gg |u|$,

so $(u + \rho g)\nabla^2 g$ will in general be small relative to $\rho\nabla g\nabla^T g$. Of course, these are somewhat loose justifications, and we may also observe that, as the sum of a positive definite and a positive semi-definite matrix, $-\nabla^2 l + \rho\nabla g\nabla^T g$ is positive definite and hence a Newton update using this approximation to the Hessian will always take us in a descent direction.

S4 Type 1 Error & Power: Additional Results

Distribution	J	$n = 10$	$n = 50$	$n = 250$
Poisson	10	0.061	0.051	0.046
Poisson	50	0.056	0.050	0.051
Poisson	250	0.049	0.056	0.050
ZINB	10	0.028	0.026	0.032
ZINB	50	0.032	0.039	0.043
ZINB	250	0.025	0.043	0.044

Table S1: Empirical type 1 error for the robust score test at the 0.05 level by simulated distribution, number of taxa J , and sample size n . Results are shown for 10,000 simulations.

Distribution	J	$n = 10$	$n = 50$	$n = 250$
Poisson	10	0.107	0.045	0.042
Poisson	50	0.159	0.069	0.053
Poisson	250	0.167	0.080	0.057
ZINB	10	0.252	0.058	0.034
ZINB	50	0.293	0.093	0.057
ZINB	250	0.307	0.098	0.059

Table S2: Empirical type 1 error for robust Wald test at the 0.05 level by simulated distribution, number of taxa J , and sample size n . Results are shown for 10,000 simulations.

Distribution	J	$n = 10$	$n = 50$	$n = 250$
Poisson	10	0.918	1.000	1.000
Poisson	50	0.718	1.000	1.000
Poisson	250	0.640	1.000	1.000
ZINB	10	0.034	0.138	0.770
ZINB	50	0.040	0.180	0.872
ZINB	250	0.028	0.194	0.908

Table S3: Empirical power for detection of smaller magnitude signal ($\beta_{kj} - g(\beta_k) = 1$) for robust score test at the 0.05 level by simulated distribution, number of taxa J , and sample size n . Results are shown for 500 simulations.

Distribution	J	$n = 10$	$n = 50$	$n = 250$
Poisson	10	0.996	1.000	1.000
Poisson	50	0.996	1.000	1.000
Poisson	250	0.992	1.000	1.000
ZINB	10	0.284	0.276	0.814
ZINB	50	0.366	0.380	0.898
ZINB	250	0.410	0.456	0.938

Table S4: Empirical power for detection of smaller magnitude signal ($\beta_{kj} - g(\beta_k) = 1$) for robust Wald test at the 0.05 level by simulated distribution, number of taxa J , and sample size n . Results are shown for 500 simulations.

Distribution	J	$n = 10$	$n = 50$	$n = 250$
Poisson	10	0.882	1.000	1.000
Poisson	50	0.986	1.000	1.000
Poisson	250	0.920	1.000	1.000
ZINB	10	0.096	0.990	1.000
ZINB	50	0.386	0.986	1.000
ZINB	250	0.276	0.922	1.000

Table S5: Empirical power for detection of larger magnitude signal ($\beta_{kj} - g(\beta_k) = 5$) for robust score test at the 0.05 level by simulated distribution, number of taxa J , and sample size n . Results are shown for 500 simulations.

Distribution	J	$n = 10$	$n = 50$	$n = 250$
Poisson	10	1.000	1.000	1.000
Poisson	50	1.000	1.000	1.000
Poisson	250	1.000	1.000	1.000
ZINB	10	0.920	1.000	1.000
ZINB	50	0.924	1.000	1.000
ZINB	250	0.962	1.000	1.000

Table S6: Empirical power for detection of larger magnitude signal ($\beta_{kj} - g(\beta_k) = 5$) over 500 simulations for robust Wald test at the 0.05 level by simulated distribution, number of taxa J , and sample size n . Results are shown for 500 simulations.

S5 Additional figures

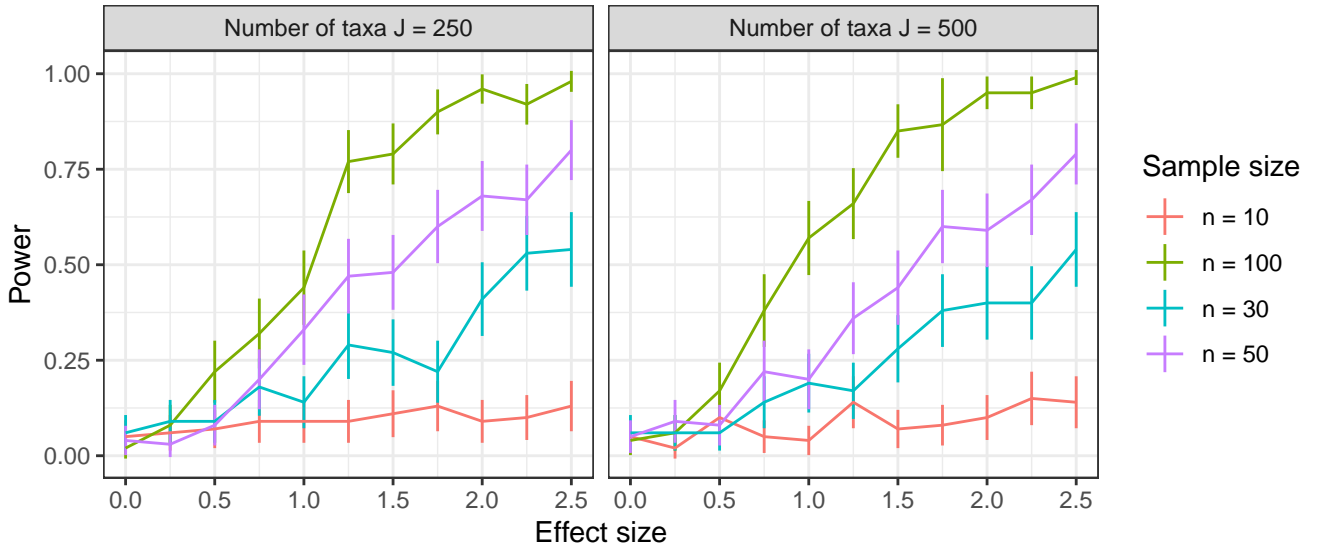


Figure S7: Empirical power to reject $\beta_{kj} = g(\beta_k)$ at the 0.05 level for zero-inflated Negative Binomial draws. Results are shown for 100 simulations. The primary purpose of these results is to provide investigators with power estimates, that can then be refined further using our simulation code.